CONF-9509216--1

LBL-37414
UC-400

Lawrence Berkeley Laboratory
UNIVERSITY OF CALIFORNIA

EARTH SCIENCES DIVISION

To be presented at the VEGAS Inauguration and Symposium, Stuttgart, Germany, September 25–27, 1995, and to be published in the Proceedings

Effective Parameters, Effective Processes: From Porous Flow Physics to *In Situ* Remediation Technology

K. Pruess

June 1995

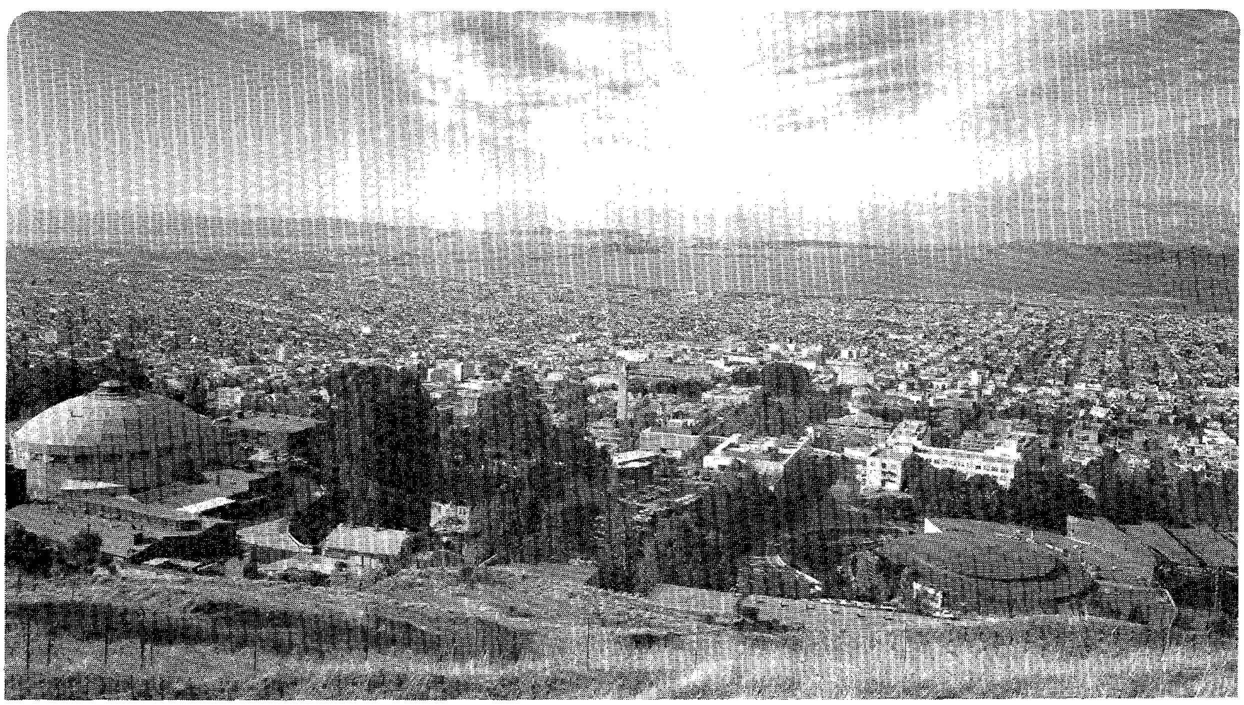

Prepared for the U.S. Department of Energy under Contract Number DE-AC03-76SF00098

DISCLAIMER

Portions of this document may be illegible in electronic image products. Images are produced from the best available original document.

LBL-37414
UC-400

Effective Parameters, Effective Processes: From Porous Flow Physics to *In Situ* Remediation Technology

Karsten Pruess

Earth Sciences Division
Lawrence Berkeley Laboratory
University of California
Berkeley, California 94720

June 1995

This work was carried out under U.S. Department of Energy Contract No. DE-AC03-76SF00098 for the Office of External Relations, administered by the Nevada Operations Office, U.S. Department of Energy, in cooperation with the Swiss National Cooperative for the Disposal of Radioactive Waste (NAGRA), and for the Director, Office of Civilian Radioactive Waste Management, Yucca Mountain Site Characterization Project Office.

Invited Paper, to be presented at
VEGAS-Symposium, Stuttgart/Germany,
September 25-27, 1995,
and to be published in the Proceedings

LBL-37414
UC-400

Effective Parameters, Effective Processes: From Porous Flow Physics to *In Situ* Remediation Technology

Karsten Pruess

Earth Sciences Division, Lawrence Berkeley Laboratory
University of California, Berkeley, CA 94720

Abstract
This paper examines the conceptualization of multiphase flow processes on the macroscale, as needed in field applications. It emphasizes that upscaling from the pore-level will in general not only introduce effective parameters but will also give rise to "effective processes," i.e., the emergence of new physical effects that may not have a microscopic counterpart. "Phase dispersion" is discussed as an example of an effective process for the migration and remediation of non-aqueous phase liquid (NAPL) contaminants in heterogeneous media. An approximate space-and-time scaling invariance is derived for gravity-driven liquid flow in unsaturated two-dimensional porous media (fractures). Issues for future experimental and theoretical work are identified.

1. Introduction
Key to the characterization of subsurface contamination conditions, and to the design and implementation of effective remediation strategies, is an understanding of the physical, chemical, and biological processes that affect the behavior of contaminants in the subsurface environment. This paper is mainly concerned with multiphase flow processes that are relevant to contamination by non-aqueous phase liquids (NAPLs), such as organic solvents and hydrocarbon fuels. The chief contaminant migration processes are: 3-phase flow of water, air, and NAPL; phase partitioning of NAPL (evaporation into the gas phase, dissolution in the aqueous phase; sorption on the solid phases); and diffusive transport in any of the phases present. Difficulties in achieving a sound mechanistic understanding of these processes arise from their inherent complexity, and from the complexity and attendant uncertainty of the hydrogeologic environment in which these processes are being played out.

2. Scale Effects
Although a detailed understanding of multiphase flow processes from first principles is desirable, even where it can be achieved it may only provide a limited basis for understanding and controlling natural systems. The difficulties arising on the typically large space and time scales encountered in the field have been variously described with catchwords such as "heterogeneity," "complexity," "upscaling", and "volume averaging." Volume-averaging of the microscopic equations for multiphase flow in porous media gives rise to complicated integrals

(Whitaker, 1986) which, for practical applications, must be replaced with phenomenological expressions. It is well accepted that description of processes on the larger field scales will generally require "effective parameters." These may differ from their laboratory-scale counterparts not only in numerical value but also conceptually, and may depend on the flow process under consideration. Examples include anisotropic effective permeability for unsaturated flow in media with stochastic heterogeneity (Yeh et al., 1985a, b, c; Mantoglou and Gelhar, 1987a, b, c), and effective or "apparent" thermal conductivities of soils that incorporate contributions from pore-scale vapor-liquid phase change processes (Cass et al., 1984).

It is not always appreciated that volume-averaging of laboratory-scale equations, such as equations for advection-diffusion processes, may not only lead to effective parameters but also to effective processes: the appearance of new terms in the governing equations that represent continuum approximations of the overall effects of microscopic processes played out in complex settings. The premier example here is hydrodynamic dispersion of solutes, i.e., the effective diffusive behavior of solutes being advected in stochastic permeability fields. The recent hydrogeology literature abounds with efforts to derive macroscopic solute dispersion from the underlying advective and mixing processes in random fields (Sahimi et al., 1986a, b; Dagan, 1988). Most work in this area has been limited to solute transport in single-phase flow. Only recently has it been recognized that analogous dispersive processes may develop during multi-phase miscible and immiscible displacements, where the dispersing quantity will be the saturation (i.e., fractional void volume) of a phase (Espedal et al., 1991; Langlo and Espedal, 1992, 1994; Pruess, 1994).

From a mathematical viewpoint, the presence of dispersive processes on a larger scale gives rise to the emergence of second-order space derivatives in the governing equations. This is what we mean by "effective process:" the emergence, through upscaling and volume averaging, of effects that may not have a microscopic counterpart. Theoretical upscaling is only one approach by which effective processes may be identified; an alternative and more direct approach would be through physical or numerical experimentation on the appropriate scale, and subsequent direct conceptualization of the phenomena. This is in fact the route that Scheidegger (1954) took when he introduced the concept of hydrodynamic dispersion, by suggesting to treat solute transport in porous media in analogy to Brownian motion.

3. Spreading of Liquid Plumes in the Vadose Zone

Localized infiltration of aqueous and non-aqueous phase liquids (NAPLs) occurs in many circumstances. Examples include leaky underground pipelines and storage tanks, landfill and disposal sites, and surface spills. If the permeability of the medium in which the spill occurs is sufficiently high the flow will be dominated by gravity effects. In this case liquids will move primarily downward, but "straight" downward flow is only possible when appropriate permeability is available in the vertical direction. Liquids flowing downward in unsaturated soils, or in large (sub-)vertical fractures, may encounter low-permeability obstacles, such as silt or clay lenses in soils, or asperity contacts between fracture walls. The liquid will then pond atop the obstacles and be diverted sideways, until other predominantly vertical pathways are reached (Fig. 1).

The conventional treatment of liquid percolation through unsaturated media includes gravity, pressure, and capillary effects. Mass flux in phase β is written as a multi-phase generalization of Darcy's law,

$$\mathbf{F}_\beta = -k\frac{k_{r\beta}}{\mu_\beta}\rho_\beta\left(\nabla P_\beta - \rho_\beta \mathbf{g}\right) \qquad (1).$$

Here k is absolute permeability, $k_{r\beta}$ is relative permeability, μ is viscosity, ρ density, P_β is pressure in phase β, and g is gravitational acceleration. Additional molecular-diffusive fluxes, not written in Eq. (1), may also be present. Horizontal flow diversion from media heterogeneities can be represented only if such heterogeneity is modeled in full explicit detail. In practical applications, explicit numerical modeling of small-scale heterogeneities would require prohibitively large numbers of grid blocks, because heterogeneities occur on many different scales. Using our general-purpose numerical simulation code TOUGH2 (Pruess, 1991), enhanced with a set of preconditioned conjugate gradient solvers (Moridis and Pruess, 1995), we have performed high-resolution numerical simulation experiments to explore whether the overall effects of heterogeneity may be approximated by means of an effective porous continuum. As an example, Fig. 2 shows a 2-D vertical section of a medium that features a random distribution of impermeable horizontal obstacles. This kind of heterogeneity structure may be encountered in shallow sedimentary soils, where the impermeable obstacles would represent shale, silt, or clay bodies (Begg et al., 1985). Detailed specifications for this system are given in Table 1. Similar parameters may also be applicable to fractures in hard rocks, in which case the obstacles would represent asperity contacts between fracture walls.

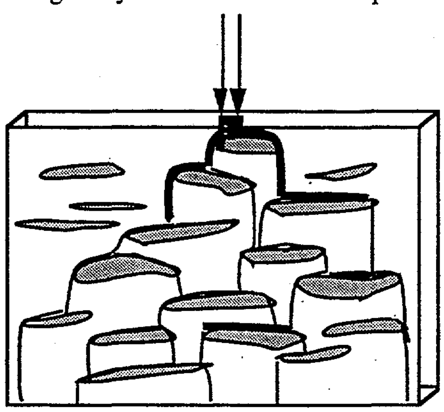

Figure 1. Schematic of liquid infiltration in an unsaturated heterogeneous medium. Regions of low permeability (shaded) divert flux sideways and cause a lateral spreading of the infiltration plume.

3.1 Numerical Simulations

From simulations of single-phase flow in the medium of Fig. 2 we find that effective horizontal and vertical permeabilities are k_h = 7.5 and k_v = 1.2 darcies, respectively (anisotropy ratio of k_h/k_v = 6.3). Emergence of a large-scale permeability anisotropy is not the only effect arising from the heterogeneities, however. A more subtle effect becomes apparent when placing a localized plume of enhanced liquid saturation into the medium, and permitting it to flow in response to gravitational force. Plume behavior is analyzed by evaluating spatial moments (Sahimi et al., 1986a, b; Freyberg, 1986; Essaid et al., 1993). An effective transverse dispersivity for a localized plume is then calculated as

$$\alpha_T = \frac{1}{2}\frac{d}{dz}\left(\sigma_T^2\right) \quad (2)$$

where z is the vertical center-of-mass coordinate of the plume, and σ_T^2 is the mean square plume size (variance) in the transverse (horizontal) direction.

Fig. 3 shows a simulated water infiltration plume in the medium of Fig. 2 for a case where capillary pressure is neglected. In this case flow proceeds in

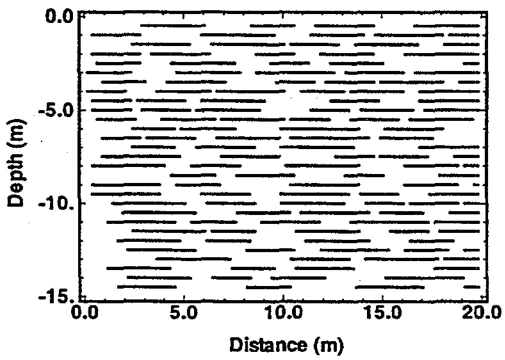

Figure 2. Two-dimensional vertical section of a heterogeneous medium with a random distribution of impermeable obstacles (black segments).

Table 1. Parameters for test problem with detailed explicit heterogeneity.

Permeability	$k = 10^{-11}$ m^2
Porosity	$\phi = 0.35$
Relative Permeability	
van Genuchten function (1980)	
irreducible water saturation	$S_{lr} = 0.15$
exponent	$\lambda = 0.457$
Capillary Pressure	
van Genuchten function (1980)	
irreducible water saturation	$S_{lr} = 0.0, 0.15$
exponent	$\lambda = 0.457$
strength coefficient	$a = 5$ m^{-1}
Geometry of Flow Domain	
2-D vertical (X-Z) section	
width (X)	20 m
depth (Z)	15 m
gridding	$\Delta X = .25$ m $\Delta Z = .125$ m
Initial Water Saturation	
for $6.5 \leq X \leq 13.5$m and $-3.5 \leq Z \leq 0$ m	$S_l = 0.99$
remainder of domain	$S_l = 0.15$

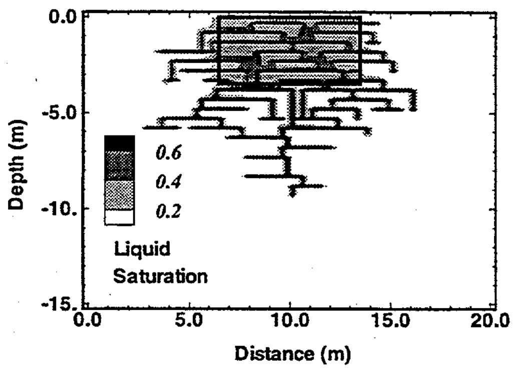

Figure 3. Simulated infiltration plume in the medium of Fig. 2 after 2×10^5 seconds, without capillary pressure. Initially, the plume has a uniform water saturation of S_l = .99 and occupies the region indicated by the black rectangle at the top of the figure.

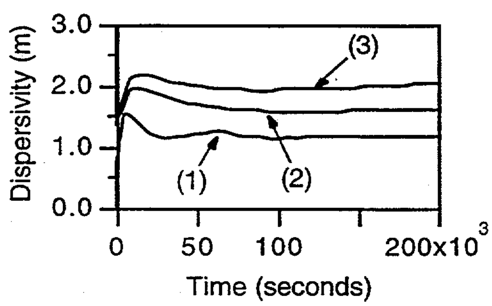

Figure 4. Transverse dispersivities for plumes with increasingly strong capillary pressures: (1) no P_{cap}, (2) moderate P_{cap} (S_{lr} = 0.0), and (3) strong P_{cap} (S_{lr} = 0.15).

the form of narrow seeps (fingers), while inclusion of capillary pressures dampens out the fingers and produces a smoother saturation distribution (not shown). Using Eq. (2) to analyze for effective transverse dispersivities we obtain the results shown in Fig. 4. It is seen that after some early-time transients, transverse dispersivities stabilize at very nearly constant values of 1.2, 1.7, and 2.0 m, respectively, for the cases of (1) no capillary pressure, (2) weaker and (3) stronger capillary pressure. These results as well as others not shown here indicate that transverse plume spreading from intrinsic heterogeneities of porous media may proceed as a Fickian diffusion process. We conclude that the heterogeneous medium of Fig. 2 behaves like an effective dispersive medium.

To represent dispersion within a continuum framework requires adding another term to the flux expression Eq. (1). The "phase-dispersive" liquid flux may be written (Pruess, 1995)

$$\mathbf{F}_{l,\mathrm{dis}} = -k \frac{\rho_l g}{\mu_l} \rho_l \alpha_T \left(\mathbf{e}_x \frac{\partial k_{rl}}{dx} + \mathbf{e}_y \frac{\partial k_{rl}}{dy} \right) \qquad (3)$$

where $\mathbf{e}_x$ and $\mathbf{e}_y$ are unit vectors in x and y-directions, respectively.

3.2 Dispersion Model

The dispersive behavior of a medium with homogeneous "background" permeability and a random distribution of embedded impermeable obstacles, such as shown in Fig. 2, can be derived from a simple model. Consider a localized seep where liquid is flowing straight downward, until a horizontal impermeable obstacle of width d is encountered. Assume that the seep splits into two seeps of equal strength which, in the center-of mass (COM) coordinate frame, are located at x = +d/2 and x = -d/2, respectively. Then the variance increases by

$$\Delta\sigma^2 = \frac{1}{2}\left\{(+d/2)^2 + (-d/2)^2\right\} = d^2/4 \tag{4}$$

In a statistically homogeneous medium, the average width of an obstacle will be independent of position, and the number of obstacles encountered will be proportional to the vertical distance traveled. Under these conditions the variance of a seep will, on average, grow linearly with vertical distance. Consequently, from Eq. (2), the associated dispersivity will be constant, i.e., the seep will be subject to a diffusion-like spreading. Denoting with τ the probability of encountering an obstacle over a vertical migration distance D, the transverse dispersivity can be expressed, using Eqs. (2, 4), as

$$\alpha_T = \frac{1}{2}\frac{\tau}{D}\frac{d^2}{4} \tag{5}$$

For the medium of Fig. 2, the obstacles have widths in the range $2 \text{ m} \le d \le 4$ m, with an average d = 2.67 m. The obstacles are randomly placed in rows with a vertical distance D = 0.5 m, and their combined length is 2/3 of the length of a row. Thus, the probability of hitting an obstacle while migrating over a vertical distance of 0.5 m is $\tau = 2/3$. Inserting these parameters into Eq. (5), we obtain $\alpha_T = 1.19$ m, in excellent agreement with the value derived from the numerical simulation (see Fig. 4).

On theoretical grounds we expect dispersion effects from medium heterogeneities and from capillarity to be additive (Pruess, 1995). The capillary dispersivity is given by (Pruess, 1994)

$$\alpha_{cap,T} = \frac{k_h}{k_v}\frac{1}{\rho_l g}\frac{dP_{cap}}{d\ln k_{rl}} \tag{6}$$

Capillary dispersivity is close to 0.5 m over a wide range of saturations for the moderately strong capillary pressure function used in our numerical plume migration experiments (Pruess, 1994). This is in excellent agreement with the difference in dispersivities seen between cases (1) and (2) in Fig. 4, confirming that heterogeneity- and capillary-derived transverse dispersivities are additive.

4. Dependence on Space and Time Scales

The migration of liquids through the unsaturated zone proceeds under the combined action of gravity, capillary, and pressure forces. Within a continuum framework, the governing equations for multiphase, multicomponent flows can be written in integral form as (Pruess, 1991)

$$\frac{d}{dt}\int_{V_n} M^{\kappa}\, dV_n = \int_{\Gamma_n} \mathbf{F}^{\kappa} \bullet \mathbf{n}\, d\Gamma_n \qquad (7)$$

Here we have for simplicity neglected sink and source terms. M^{κ} is the mass of component κ per unit porous medium volume, $\mathbf{F}^{\kappa}$ is the mass flux of component κ, V_n is an arbitrary subdomain of the flow system under study, Γ_n is the closed surface bounding V_n, and $\mathbf{n}$ is the unit normal pointing into V_n. Both M^{κ} and $\mathbf{F}^{\kappa}$ include a sum over all phases in which component κ may be present. We are interested in the behavior of multiphase systems under a change of space and time scales. For simplicity consider a two-dimensional heterogeneous porous medium, such as a sub-vertical fracture in hard rock with negligible matrix permeability. Let us apply a simultaneous scaling to time t and to horizontal and (sub-)vertical space coordinates, x and z, respectively

$$\begin{aligned} t &\rightarrow t' = \lambda_t \cdot t \\ x &\rightarrow x' = \lambda_x \cdot x \\ z &\rightarrow z' = \lambda_z \cdot z \end{aligned} \qquad (8)$$

Under the transformation Eq. (8), subdomain volumes scale by $\lambda_x \lambda_z$, so that the left hand side (l.h.s.) of Eq. (7) scales by $\lambda_x \lambda_z/\lambda_t$. On the r.h.s., scaling behavior is different for horizontal and vertical areas, and is also different for gravity-driven flow as compared to capillary- or pressure-driven flow. Interface areas for horizontal and vertical flow scale by λ_z and λ_x, respectively. The gravity (body force) flux term remains unchanged under the scaling Eq. (8), while pressure and capillary-driven fluxes, being proportional to (capillary) pressure gradients, scale as $1/\lambda_x$ and $1/\lambda_z$ for horizontal and vertical components, respectively. The expressions resulting from moving all scaling factors arising from the transformation Eq. (8) to the l.h.s. of Eq. (7) are shown in Table 2. To obtain scaling invariance, space and time scale factors must be chosen in such a way that the expressions given in Table 2 are equal to 1. It is seen that this cannot be achieved simultaneously for (capillary) pressure and gravity terms. Therefore, flow processes involving these different driving forces simultaneously will be different on different scales. However, an approximate scaling invariance may hold when dense liquids percolate downward in an unsaturated medium. For such flows the gas phase may be considered a passive bystander at constant pressure. For the liquid phase horizontal

Table 2: Scale factors for flow equations.

components flow terms	horizontal	vertical
capillary and pressure	λ_x^2/λ_t	λ_z^2/λ_t
gravity	-	λ_z/λ_t

flows are driven solely by pressure and capillary forces, while (sub-) vertical flows are dominated by gravity. If capillary and pressure forces on vertical flux components are small relative to gravity effects, an approximate invariance will hold if $\lambda_x{}^2/\lambda_t = \lambda_z/\lambda_t = 1$, i.e.,

$$\lambda_t = \lambda_x{}^2 = \lambda_z \qquad (9).$$

Numerical simulation experiments were performed to test the approximate scaling relationship Eq. (9). Fig. 5 shows a two-dimensional heterogeneous medium that was generated with geostatistical techniques to represent "small" fractures in hard rock. It features fairly short-range spatial correlations and numerous asperity contacts (regions of zero permeability) where the fracture walls are in contact. Apart from the different permeability structures, problem parameters are as given in Table 1. Strength of capillary pressure was scaled consistently with permeability (Leverett, 1941), i.e., $P_{cap}(k') = P_{cap}(k)\bullet\sqrt{k/k'}$. Flow simulations were then performed by placing a square liquid plume of saturation $S_l = 0.99$ at the top, center, of the domain, and letting it migrate under the combined action of gravity, capillary, and pressure forces. The liquid plume after 10^5 seconds is shown in Fig. 6. Another simulation was performed for a scaled flow system with $\lambda_x = 5$, and $\lambda_z = \lambda_t = 25$, as required by Eq. (9). Fig. 7 shows the liquid plume in the scaled system after the scaled time (25×10^5 seconds). Comparison with Fig. 6 shows that the two plumes are

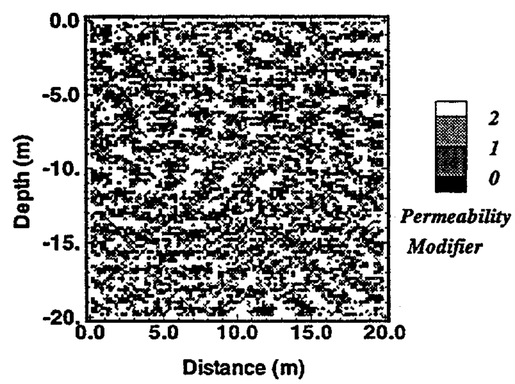

Figure 5. Stochastic permeability field, with correlation lengths of $\zeta_x = 0.2$ m, $\zeta_z = 0.1$ m.

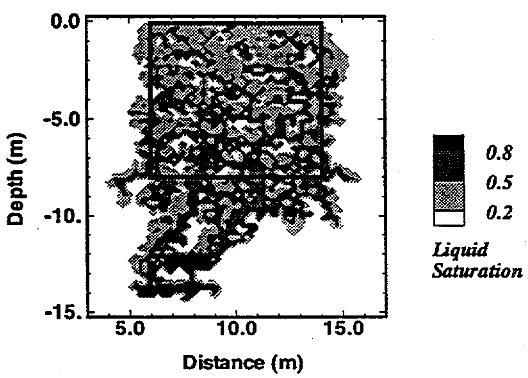

Figure 6. Simulated liquid infiltration plume in the medium of Fig. 5, after 10^5 seconds. The black square indicates the region originally occupied by the plume.

very similar, although minor differences are also apparent. This confirms the validity of the approximate scaling relationship Eq. (9) for the particular flow system and process considered here.

5. Discussion and Conclusions

In the simulations presented above water was used as the liquid phase, but similar results would be obtained for NAPL migration in the unsaturated zone. Dispersivities from permeability heterogeneity would be the same for water and NAPLs, while capillary effects would be weaker for the latter. Phase dispersion effects are therefore expected to be relatively more prominent for NAPLs.

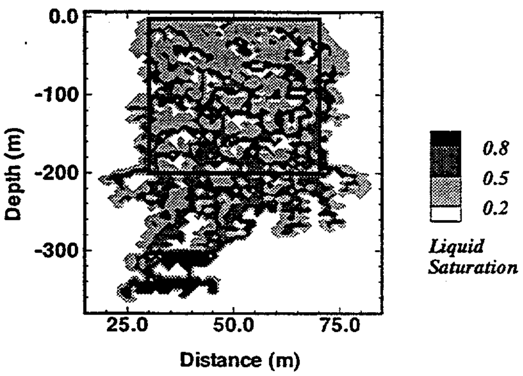

Figure 7. As Fig. 6, but for scaled flow system with $\lambda_x = 5$, $\lambda_z = 25$, after 25 x 10^5 seconds.

The phase dispersion and scaling analyses in this paper were made for two-dimensional porous media, so that they are immediately applicable only to flow in fractures, and to conditions where flow can be approximated as proceeding in 2-D vertical sections. It would be of interest to generalize these analyses to 3-D media. Fickian-type dispersive behavior from medium heterogeneities is by no means inevitable or universal. In fact, for certain heterogeneity conditions and spatial scales infiltration plumes may show "antidispersive" behavior, becoming more narrowly focused with depth (Kung, 1990). Laboratory and field experiments are needed to evaluate the range of heterogeneity conditions that would give rise to dispersive plume spreading, and to examine the validity of the space- and time-scaling invariance proposed above.

NAPL remediation techniques such as soil vapor extraction, or surfactant-enhanced solubilization and extraction, must rely for their efficiency on interphase mass transfer between the NAPL phase on the one hand, gaseous and aqueous phases on the other. Interphase mass transfer depends on small-scale details of NAPL phase distribution, such as the contact area between NAPL and surrounding phases. At small (irreducible) saturations NAPLs are not spread out volumetrically throughout the pore space; rather, they are present as thin threads, called "ganglia", whose length and thickness typically may be of the order of 1 m and 1 mm, respectively (Hunt et al., 1988). This will cause limitations for interphase mass transfer, and may seriously limit the rate at which NAPL may be removed. It is obvious that these kinds of details cannot be predicted from continuum approaches to flow.

In order to achieve engineering control over remediation processes, it may be necessary to employ several different conceptualizations of the flow system simultaneously, so that process aspects on different scales may be resolved. Volume-averaged continuum models can be used to evaluate overall migration of the contaminant plume, and to assess and achieve adequate volumetric coverage for a remediation process. More detailed models, perhaps going down to pore-level phenomena, may be needed to describe the actual distribution of NAPL and its interaction with surrounding gas and aqueous phases, or heat. It may even be possible to combine the large-scale volume-averaging approach with a detailed description of NAPL seeps and ganglia, using statistical techniques borrowed from petroleum reservoir engineering (Chesnut, 1992). Only through imaginative use of different conceptualizations for phenomena on different scales, closely coupled with experiments and site characterization efforts, will it be possible to devise and implement effective remediation strategies.

Acknowledgement

The author thanks Emilio Antunez for assistance with the generation of heterogeneous fields, and Curt Oldenburg and George Moridis for a careful review of the manuscript. This work was carried out under U.S. Department of Energy Contract No. DE-AC03-76SF00098 for the Office of External Relations, administered by the Nevada Operations Office, U.S. Department of Energy, in cooperation with the Swiss National Cooperative for the Disposal of Radioactive Waste (NAGRA), and for the Director, Office of Civilian Radioactive Waste Management, Yucca Mountain Site Characterization Project Office.

References

Begg, S.H., D.M. Chang, and H.H. Haldorsen. A Simple Statistical Method for Calculating the Effective Vertical Permeability of a Reservoir Containing Discontinuous Shales, paper SPE-14271, presented at the 60th Annual Technical Conference and Exhibition of the Society of Petroleum Engineers, Las Vegas, NV, September 1985.

Cass, A., G.S. Campbell and T.L. Jones. Enhancement of Thermal Water Vapor Diffusion in Soil. *Soil Sci. Soc. Am. J.*, Vol. 48, no. 1, pp. 25 - 32, 1984.

Chesnut, D.A. Characterizing the Altered Zone at Yucca Mountain: The Beginning of a Testing Strategy. Proceedings, Third High Level Radioactive Waste Management International Conference, Las Vegas, NV, Vol. 1, pp. 1026 - 1039, American Nuclear Society, La Grange Park, IL, April 12-16, 1992.

Dagan, G. Time-Dependent Macrodispersion for Solute Transport in Anisotropic Heterogeneous Aquifers, *Water Res. Res.*, 24 (9), 1491-1500, 1988.

Espedal, M. S., P. Langlo, O. Saevareid, E. Gislefoss and R. Hansen. Heterogeneous Reservoir Models: Local Refinement and Effective Parameters, paper SPE-21231, presented at Society of Petroleum Engineers 11th Symposium on Reservoir Simulation, Anaheim, CA, February 1991.

Essaid, H.I., W.N. Herkelrath and K.M. Hess. Simulation of Fluid Distributions Observed at a Crude Oil Spill Site Incorporating Hysteresis, Oil Entrapment, and Spatial Variability of Hydraulic Properties, Water *Res. Res.*, 29 (6), 1753-1770, 1993.

Freyberg, D.L. A Natural Gradient Experiment on Solute Transport in a Sand Aquifer. 2. Spatial Moments and the Advection and Dispersion of Nonreactive Tracers, *Water Res. Res.*, 22 (13), 2031-2046, 1986.

Hunt, J. R., N. Sitar and K. S. Udell. Nonaqueous Phase Liquid Transport and Cleanup, 1. Analysis of Mechanisms. *Water. Res. Res.*, 24 (8), 1247-1258, 1988.

Kung, K. J. S. Preferential Flow in a Sandy Vadose Zone: 2. Mechanism and Implications, *Geoderma*, Vol. 46, pp. 59-71, 1990.

Langlo, P. and M.S. Espedal. Heterogeneous Reservoir Models, Two-Phase Immiscible Flow in 2-D, in T.F. Russell et al. (eds.), *Computational Methods in Water Resources IX,* Vol. 2, pp. 71-79, Elsevier, London, New York, 1992.

Langlo, P. and M.S. Espedal. Macrodispersion for Two-Phase, Immiscible Flow in Porous Media. *Adv. Wat. Res.*, Vol. 17, pp. 297 - 316, 1994.

Leverett, M. C., Capillary Behavior in Porous Solids, *Trans. Soc. Pet. Eng. AIME*, 142, 152-169, 1941.

Mantoglou, A. and L.W. Gelhar. Stochastic Modeling of Large-Scale Unsaturated Flow Systems. *Water Res. Res.,* 23 (1), 37 - 46, 1987a.

Mantoglou, A. and L.W. Gelhar. Capillary Tension Head Variance, Mean Soil Moisture Content, and Effective Specific Soil Moisture Capacity of Transient Unsaturated Flow in Stratified Soils. *Water Res. Res.*, 23 (1), 47 - 56, 1987b.

Mantoglou, A. and L.W. Gelhar. Effective Hydraulic Conductivities of Transient Unsaturated Flow in Stratified Soils. *Water Res. Res.,* 23 (1), 57 - 67, 1987c.

Moridis, G. and K. Pruess. Flow and Transport Simulations Using T2CG1, a Package of Conjugate Gradient Solvers for the TOUGH2 Family of Codes. Lawrence Berkeley Laboratory Report LBL-36235, Lawrence Berkeley Laboratory, Berkeley, CA, 1995.

Pruess, K. TOUGH2 - A General Purpose Numerical Simulator for Multiphase Fluid and Heat Flow. Report No. LBL-29400, Lawrence Berkeley Laboratory, Berkeley, CA, May 1991.

Pruess, K. On the Validity of a Fickian Diffusion Model for the Spreading of Liquid Infiltration Plumes in Partially Saturated Heterogeneous Media. Invited Paper, in: *Computational Methods in Water Resources X,* Vol. 1, pp. 537 - 544, Kluwer Academic Publishers, Dordrecht, Boston, London, 1994.

Pruess, K. A Fickian Diffusion Model for the Spreading of Liquid Plumes Infiltrating in Heterogeneous Media. in press in *Transport in Porous Media,* 1995.

Sahimi, M., B. D. Hughes, L. E. Scriven and H. T. Davis. Dispersion in Flow Through Porous Media - I. One-Phase Flow. *Chem. Eng. Sci.*, Vol. 41, No. 8, pp. 2103-2122, 1986a.

Sahimi, M., A. A. Heiba, H. T. Davis and L. E. Scriven. Dispersion in Flow Through Porous Media - II. Two-Phase Flow. *Chem. Eng. Sci.*, Vol. 41, No. 8, pp. 2123-2136, 1986b.

Scheidegger, A. E. Statistical Hydrodynamics in Porous Media. *J. Appl. Phys.*, 25 (8), 994-1001, 1954.

van Genuchten, M. Th. A Closed-Form Equation for Predicting the Hydraulic Conductivity of Unsaturated Soils, *Soil Sci. Soc. Am. J.*, Vol. 44, pp. 892-898, 1980.

Whitaker, S. Flow in Porous Media II: The Governing Equations for Immiscible Two-Phase Flow. *Transport in Porous Media*, Vol. 1, pp. 105 - 125, 1986.

Yeh, T.C.J., L.W. Gelhar, and A.L. Gutjahr. Stochastic Analysis of Unsaturated Flow in Heterogeneous Soils, 1, Statistically Isotropic Media. *Water Res. Res.*, 21 (4), 447 - 456., 1985a.

Yeh, T.C.J., L.W. Gelhar, and A.L. Gutjahr. Stochastic Analysis of Unsaturated Flow in Heterogeneous Soils, 2, Statistically Anisotropic Media with Variable α. *Water Res. Res.*, 21 (4), 457 - 464, 1985b.

Yeh, T.C.J., L.W. Gelhar, and A.L. Gutjahr. Stochastic Analysis of Unsaturated Flow in Heterogeneous Soils, 3, Observations and Applications. *Water Res. Res.*, 21 (4), 465 - 471, 1985c.